Phytochemistry xxx (2014) xxx–xxx

Contents lists available at ScienceDirect

Phytochemistry

journal homepage: www.elsevier.com/locate/phytochem

Pinoresinol reductase 1 impacts lignin distribution during secondary cell wall biosynthesis in Arabidopsis

Qiao Zhao [a], Yining Zeng [b,e], Yanbin Yin [c], Yunqiao Pu [d,e], Lisa A. Jackson [a,e], Nancy L. Engle [e,f], Madhavi Z. Martin [e,f], Timothy J. Tschaplinski [e,f], Shi-You Ding [b,e], Arthur J. Ragauskas [d,e], Richard A. Dixon [a,e,g,*]

[a] Plant Biology Division, Samuel Roberts Noble Foundation, 2510 Sam Noble Parkway, Ardmore, OK 73401, USA
[b] Biosciences Center, National Renewable Energy Laboratory, Golden, CO 80401, USA
[c] Department of Biological Sciences, Northern Illinois University, DeKalb, IL 60115, USA
[d] Institute of Paper Science and Technology, Georgia Institute of Technology, Atlanta, GA, USA
[e] BioEnergy Science Center (BESC), Oak Ridge National Laboratory, Oak Ridge, TN 37831, USA
[f] Biosciences Division, Oak Ridge National Laboratory, Oak Ridge, TN 37831, USA
[g] Department of Biological Sciences, University of North Texas, Denton, TX 76203, USA

ARTICLE INFO

Article history:
Available online xxxx

Keywords:
Lignan
Lignin
Interfascicular fiber
Mutant
Stimulated Raman scattering microscopy

ABSTRACT

Pinoresinol reductase (PrR) catalyzes the conversion of the lignan (−)-pinoresinol to (−)-lariciresinol in *Arabidopsis thaliana*, where it is encoded by two genes, *PrR1* and *PrR2*, that appear to act redundantly. *PrR1* is highly expressed in lignified inflorescence stem tissue, whereas *PrR2* expression is barely detectable in stems. Co-expression analysis has indicated that *PrR1* is co-expressed with many characterized genes involved in secondary cell wall biosynthesis, whereas *PrR2* expression clusters with a different set of genes. The promoter of the *PrR1* gene is regulated by the secondary cell wall related transcription factors SND1 and MYB46. The loss-of-function mutant of *PrR1* shows, in addition to elevated levels of pinoresinol, significantly decreased lignin content and a slightly altered lignin structure with lower abundance of cinnamyl alcohol end groups. Stimulated Raman scattering (SRS) microscopy analysis indicated that the lignin content of the *prr1-1* loss-of-function mutant is similar to that of wild-type plants in xylem cells, which exhibit a normal phenotype, but is reduced in the fiber cells. Together, these data suggest an association of the lignan biosynthetic enzyme encoded by *PrR1* with secondary cell wall biosynthesis in fiber cells.

1. Introduction

Lignans are dimers derived from the stereospecific oxidative coupling of hydroxycinnamyl alcohols. The initial step of lignan dimerization is mediated by an oxidase (e.g. laccase) acting in concert with a dirigent protein that confers enantio-selectivity to the free radical-derived coupling (Davin et al., 1997). Approximately 3000 different lignans are widely distributed in the plant kingdom (Schmidt et al., 2010). The numerous beneficial effects of lignans on human health, via estrogenic and anticancer activities, are well documented (Dixon, 2004; McCann et al., 2005). However, the exact roles of lignans *in planta* remain elusive although it has been hypothesized that they are involved in plant defense (Naoumkina et al., 2010).

The most characterized lignans are the group with 9(9′)-oxygen linkages (Umezawa, 2003). This class of lignans arises from the enantio-selective dimerization of two coniferyl alcohol units (**1**) to give rise to pinoresinol (**2**). Pinoresinol is then sequentially reduced to lariciresinol (**3**) and secoisolariciresinol (**4**) by a bi-functional pinoresinol/lariciresinol reductase (PLR) (Nakatsubo et al., 2008; Umezawa, 2003). Because of its stereo-selectivity, PLR is suggested to have enantiomeric control on the lignan biosynthetic pathway even though the dirigent protein is considered to be the asymmetric inducer (von Heimendahl et al., 2005). Conventional PLRs can utilize both pinoresinol and lariciresinol as substrates (i.e. are bifunctional) (Hano et al., 2006; von Heimendahl et al., 2005). However, in *Arabidopsis thaliana*, the two pinoresinol reductase enzymes show only weak or no activity toward lariciresinol, and are therefore named PrR1 and PrR2 rather than PLR (Nakatsubo et al., 2008).

* Corresponding author. Present address: Department of Biological Sciences, University of North Texas, 1155 Union Circle #305220, Denton, TX 76203-5017, USA. Tel.: +1 940 565 2308.
E-mail address: Richard.Dixon@unt.edu (R.A. Dixon).

http://dx.doi.org/10.1016/j.phytochem.2014.07.008
0031-9422/

PLR genes have organ-specific expression patterns. In flax (*Linum usitatissimum*), genes encoding two PLRs with different enantiospecificity have been cloned. Both Lu*PLR1* and Lu*PLR2* are expressed in flax seed tissues, whereas only Lu*PLR2* is expressed in stem and leaf tissues (Hemmati et al., 2010). In Arabidopsis, both PrR1 and PrR2 catalyze pinoresinol reduction in a redundant manner in root tissue, where lignans are mostly accumulated, but only PrR1 is active in stem tissue (Nakatsubo et al., 2008).

The basic unit of pinoresinol, coniferyl alcohol, is also shared by the lignin biosynthesis pathway. Lignin is the second most abundant biopolymer on earth, and a major component of plant secondary cell walls. It is derived from three major subunit precursors; so-called H (*p*-coumaryl alcohol), G (coniferyl alcohol) and S (syringyl alcohol) monolignols (Bonawitz and Chapple, 2010; Zhao and Dixon, 2011). Even though coniferyl alcohol is the common unit of both lignin and lignans, there is no evidence that lignans *per se* are components of the plant wall structure. It is also not clear how plants allocate coniferyl alcohol for the biosynthesis of lignans versus lignin.

Recently, it has been shown in both flax and pine that the lignan-related gene *PLR* is up-regulated along with cell wall biosynthetic genes in highly lignifying stem tissues or during compression wood formation (Huis et al., 2012; Villalobos et al., 2012). Furthermore, a comparison of co-expressed gene networks with primary and secondary wall cellulose synthases in a variety of different plant species identified gene families that are consistently co-regulated with cellulose biosynthesis; among these genes was *PrR1* (Ruprecht et al., 2011). Because Arabidopsis PrR1 is only expressed highly in mature stem tissue, we have further investigated the potential role of this gene in cell wall biosynthesis. Our results confirm that *PrR1* is co-expressed with secondary cell wall biosynthetic genes, indicate directly that *PrR1* is regulated by regulators of secondary cell wall formation, and show that loss of function of *PrR1* results not only in changes in lignin levels, but also in alterations in lignin structure and tissue-specific lignin distribution.

2. Results

2.1. Differential expression of PrR1 and PrR2 in Arabidopsis

The different gene expression patterns of *PrR1* and *PrR2* were confirmed by analysis of microarray expression data from the Arabidopsis eFP Browser; *PrR1* transcripts are expressed in most tissues, with highest level in the lignified second internodes (Fig. S1), whereas *PrR2* transcript levels are high in root tissues, where most lignan accumulates, with almost no transcripts detectable in the 2nd internode (Fig. S2).

To investigate genes which are co-expressed with *PrR1* and *PrR2*, we examined the recently built cell wall co-expression database (http://csbl.bmb.uga.edu/publications/materials/shanwang/CWRPdb/index.html; Wang et al., 2012). A bi-clustering analysis of Arabidopsis microarray data with a focus on cell wall-related genes was applied to build co-expressed gene modules. In each module graph, the node is shown as a yellow diamond (known/annotated cell wall-related genes), an aquamarine square (known/annotated transcription factor genes) or a red circle (other genes); an edge connecting two nodes means that these two genes are co-expressed (Fig. 1). Similar co-expression graphs are also available in the ATTED-II database (http://atted.jp/data/locus/At4g13660.shtml), which uses different methods for clustering microarray data and calling co-expression modules.

Based on this analysis, *PrR1* is co-expressed with many characterized cell wall-related genes represented by yellow diamonds and aquamarine squares (Fig. 1). For instance, *LAC17* is a laccase that has been directly implicated in lignin biosynthesis (Berthet et al., 2011); cellulose synthase-like A9 (*CSLA9*) is a beta-mannan

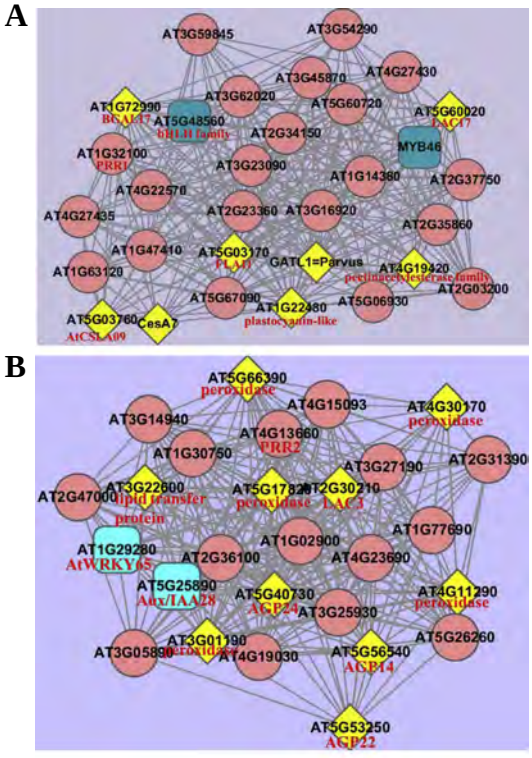

Fig. 1. Gene co-expression networks for Arabidopsis PrR1 and PrR2. (A) PrR1 is co-expressed with many known secondary cell wall biosynthetic genes. (B) PrR2 is co-expressed with an entirely different set of genes.

synthase involved in hemicellulose biosynthesis (Davis et al., 2010); cellulose synthase A7(*CesA7*) is involved in cellulose synthesis and *MYB46* is a transcriptional master switch of secondary cell wall formation (Zhong et al., 2007). These data confirm the co-expression of *PrR1* with *CesA* genes as previously reported (Ruprecht et al., 2011). In contrast, *PrR2* clusters with a totally different set of genes, including a laccase that has not been implicated in lignin polymerization, one peroxidase that has been implicated in lignin biosynthesis (Fig. 1; Table S1) and a protein associated with casparian strip formation, a process which involves peroxidase-mediated lignification in specific cell types in the root (Lee et al., 2013).

2.2. PrR1 is regulated by the secondary cell wall transcription factors SND1 and MYB46

To investigate whether *PrR1* is under the control of secondary wall transcription factors, we used an Arabidopsis leaf protoplast-based promoter *trans*-activation system. Protoplasts were transfected with a construct in which firefly luciferase (reporter) is driven by the promoter consisting of a 1 kb DNA fragment upstream of the start codon of *PrR1*. SND1 and MYB46 were chosen as potential trans-activators for this assay since both are known to be master switches of the entire secondary cell wall biosynthetic program (Zhong et al., 2006, 2007). Co-expression of cauliflower mosaic virus (CaMV) 35S promoter driven SND1 or MYB46 activated the expression of the firefly luciferase reporter gene driven by the *PrR1* promoter by around 30-fold (Fig. 2).

2.3. Loss of function of PrR1 affects both lignan and lignin biosynthesis

The *prr1-1* knock-out mutant SALK_058467 was obtained from the ABRC at Ohio State University (http://abrc.osu.edu/) (Nakatsubo et al., 2008). This line contains a T-DNA insertion

Please cite this article in press as: Zhao, Q., et al. Pinoresinol reductase 1 impacts lignin distribution during secondary cell wall biosynthesis in Arabidopsis. Phytochemistry (2014), http://dx.doi.org/10.1016/j.phytochem.2014.07.008

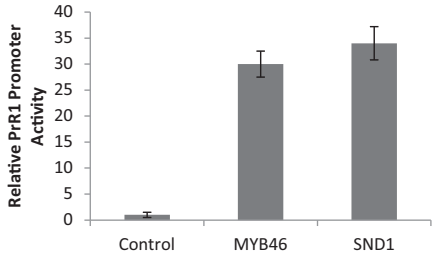

Fig. 2. The *PrR1* promoter is regulated by the SND1 and MYB46 transcription factors in protoplast transactivation assays. A PrR1 promoter-luciferase construct and effector constructs (35S: transcription factor) were co-transfected into protoplasts, along with a Renilla luciferase gene driven by the 35S promoter for correction for transfection efficiency.

within an exonic region of the *PrR1* gene. Mature inflorescence tissue was harvested and subjected to metabolite profiling by gas chromatography–mass spectrometry (GC–MS). The results (Table 1) indicate that the concentration of the lignan, pinoresinol, was 4.8-fold higher in the loss-of-function *prr1* mutant than in control plants. At the same time, the concentrations of sinapic acid and its conjugation storage product, sinapoyl-malate, were reduced to 80% and 50% of the control, respectively. The putative product of PrR1, lariciresinol, was not present at detectable levels in any of the plant lines. Although the vast majority of metabolites were not altered in *prr1*, a limited number of nitrogenous metabolites were reduced 17–29%, including ethanolamine, glutamine, and β-alanine, Whereas sinapic acid was modestly reduced in the loss-of-function mutant, it was increased (1.36-fold) in the PrR1 over-expression line, as was dehydroconiferyl alcohol, 4-*O*-glucopyranosyl-vanillic acid (1.26×) and three coniferyl alcohol-derived unidentified lignans (eluting at 16.48, 16.53, and 17.17 min, ~1.4×). These data are consistent with a role for PrR1 in lignan biosynthesis in the Arabidopsis stem. The metabolite responses observed in the over-expression line suggest a more generalized function in the production of guaiacyl-derived lignans.

Next, lignin content and composition of the *prr1* loss-of-function mutant were determined. Thioacidolysis analysis, which measures primarily β-*O*-4-linked monolignol units, revealed that the mutant had a small but significant reduction in thioacidolysis yield compared to the wild-type (Fig. 3), with similar reductions in the proportions of both G and S monolignol units.

To further compare lignin composition in the *prr1* loss-of-function mutant and wild type, lignin was extracted and subjected to nuclear magnetic resonance spectroscopy. Analysis of ^{13}C–^{1}H HSQC spectra revealed similar carbon–proton correlation signal patterns in both the aromatic and aliphatic regions of the lignin from the wild type and *prr1* mutant, indicative of no significant changes in lignin core structures (Fig. 4). The aromatic carbons in syringyl and guaiacyl units were readily observed with the presence of their diagnostic correlation signals around 103.8/6.67 ($S_{2/6}$), 110.5/6.94 (G_2), 114.8/6.88 (G_5), and 118.6/6.81 (G_6) ppm, respectively. Substructures A–E (Fig. 4) were evidently detected in the lignin from both wild type and *prr1* mutant, with β-*O*-4, phenylcoumaran and resinol being the major inter-linkage subunits. The semiquantitative analysis of subunit contours in HSQC spectra showed that the lignin in the mutant appeared to have a slightly higher relative abundance of β-*O*-4 linked subunits (A in Fig. 4). More clearly, the signal intensities of dibenzodioxocin and cinnamyl alcohol end groups were notably decreased in the *prr1* mutant.

2.4. Impact of loss of function of PrR1 on the cellular distribution of lignin

The above analyses of lignin determined the thioacidolysis yield and composition of the polymer in the bulk lignin, i.e. the sum of the lignin from all cell types. The SND1 transcription factor that regulates PrR1 primarily controls lignification in interfascicular fibers (Zhao et al., 2010a; Zhong et al., 2006). We therefore reasoned that additional information on the impacts of loss of *PrR1* function on lignification could be obtained by examination of tissue-specific changes in lignin composition. We have previously employed laser capture microdissection for this purpose in the model legume *Medicago truncatula* (Nakashima et al., 2008). However, this approach is extremely time-consuming. We therefore decided to use two-color stimulated Raman scattering microscopy (SRS), which has been utilized for *in situ* quantification of lignin and polysaccharides at both the tissue- and cell-specific level (Ding et al., 2012). Under the light microscope, the cell size and cell wall thickness of secondarily thickened cells in the second internode of the stem appear to be similar in wild type and mutant. The lignin contents of xylem fibers and vessel cells were imaged using SRS microscopy and the average lignin intensities were compared (Fig. 5A and B). Interestingly, the mutant exhibits a significant reduction in lignin content in the fibers, but not in the vessel cells, as seen when lignin distribution across the cell wall is presented as pixel intensity and normalized to the sum of all intensities (Fig. 5C). In xylem vessels, the lignin distribution is similar in wild-type and mutant plants (Fig 5A), whereas in xylem fibers, the lignin signal peak shifted to lower intensity and narrower intensity distribution across the cell wall in the mutant compared with wild type (Fig. 5B). Analysis of SRS signals across larger cross-sectional areas of the first, second and third internodes of the inflorescence stems did not reveal an increase in collapsed xylem vessels, as previously reported for this mutant (Ruprecht et al., 2011) (Fig. S3).

Total cell wall carbohydrate content was also compared between the mutant and wild type using two-color SRS microscopy. In both fibers and vessel cells, the mutant has a reduced level of carbohydrate, and the difference is more striking in fibers (Fig. 5D).

2.5. Changes in gene expression as a result of altering PrR1 expression

The lignan dehydrodiconiferyl alcohol has been ascribed a role in the control of plant development, specifically as a regulator of cell division (Binns et al., 1987). It is therefore possible that the observed impacts of modification of PrR1 expression on cell wall composition/structure could be secondary effects resulting from altered plant development rather than direct effects associated with lignin precursor synthesis. If PrR1 were involved in the biosynthesis of a lignan metabolite with a regulatory function, it is likely that loss of *PrR1* function would have an impact on many genes controlled by that regulator. To determine whether loss of function of *PrR1* causes major changes in gene expression, we performed microarray analysis. Compared with wild type, only very few genes are up-regulated or down-regulated by over twofold as a result of *PrR1* disruption. Among those, only one gene (At3g44990, encoding a xyloglucan endo-transglycosylase), has a functionally identified role in cell wall biosynthesis (Table S2), and none of the genes was strongly up- or down-regulated. We also examined the effects of over-expression of PrR1 by microarray analysis. A fourfold over-expression of PrR1 was associated with over twofold expression of 59 genes, none of which appeared to be directly associated with cell wall biosynthesis (Table S3). In fact, the majority of the up-regulated genes were annotated as being involved in abiotic stress responses (Table S3). Note that the extent of up-regulation of genes as a result of *PrR1* over-expression was, overall, much greater than in response to loss of function of *PrR1* (Tables S2 and S3).

3. Discussion

Lignin is a phenylpropanoid polymer that serves as one of the major secondary cell wall components. Dimerization of two units

Please cite this article in press as: Zhao, Q., et al. Pinoresinol reductase 1 impacts lignin distribution during secondary cell wall biosynthesis in Arabidopsis. Phytochemistry (2014), http://dx.doi.org/10.1016/j.phytochem.2014.07.008

Table 1
Metabolite concentrations (μg/g DW sorbitol equivalent) of shoot biomass of *Arabidopsis thaliana* wild-type (WT), *prr1* loss-of-function mutant (*prr1*), and PrR1 overexpression plants (PrR1). The average (Avg) concentration of two biological replicates per plant type is shown. Unknowns are identified by their retention time followed by key mass-to-charge ratios (*m*/*z*).

Plant type Metabolite	*prr1* Avg	WT Avg	PrR1 Avg	Fold change prr1/WT	Fold change PrR1/WT
4-Hydroxyphenylethanol	1.1	0.6	2.1	1.70	3.31
Raffinose	48.5	37.5	82.5	1.29	2.20
Galactinol	117.5	63.2	134.6	1.86	2.13
Glutamic acid	642.3	508.6	818.2	1.26	1.61
13.53 140 342	18.5	15.9	25.3	1.17	1.60
Maltose	199.6	180.7	288.3	1.10	1.59
Sinapyl aldehyde	3.5	2.7	4.2	1.30	1.57
Digalactopyranosylglycerol	7.8	7.4	11.3	1.05	1.53
Monopalmitin	63.2	58.6	87.3	1.08	1.49
Coniferyl aldehyde	2.8	2.4	3.5	1.18	1.48
16.53 361 guaiacyl lignan	2.5	3.5	5.0	0.72	1.42*
16.48 guaiacyl lignan	1.6	2.2	3.1	0.73	1.40*
cis-Sinapic acid	54.7	68.4	94.9	0.80*	1.39
17.07 498 588 558	0.21	0.32	0.44	0.67	1.38*
Monostearin	4.7	3.6	4.9	1.32	1.38
16.57 guaiacyl lignan	1.0	1.3	1.8	0.71	1.37
17.17 320 guaiacyl lignan	2.2	3.3	4.5	0.68	1.37*
Syringic acid-4-O-glucoside	4.6	5.9	7.9	0.78	1.36
trans-Sinapic acid	207.1	258.9	351.3	0.80*	1.36*
Coniferyl alcohol	5.5	5.8	7.8	0.95	1.35
Alpha-Tocopherol	1.0	1.0	1.3	1.00	1.35
Galactopyranosylglycerol	41.1	33.2	43.8	1.24	1.32
p-Toluic acid	3.6	1.6	2.1	2.21	1.31
14.73 267 guaiacyl lignan	1.9	2.1	2.7	0.92	1.30
a,a-Diglycerol-phosphate	56.1	54.7	70.8	1.03	1.29
Xylitol	10.6	9.2	11.8	1.15	1.28
1-Linoleyl-rac-glycerol	11.4	11.1	14.3	1.03	1.28
Dehydroconiferyl alcohol	0.19	0.29	0.36	0.65	1.26*
Gamma-Aminobutyric acid	328.4	291.2	367.1	1.13	1.26
Vanillic acid	3.3	3.5	4.3	0.95	1.25
Vanillic acid-4-O-glucoside	46.6	52.3	65.4	0.89	1.25*
Vanillin	1.9	2.1	2.6	0.88	1.24
Threonic acid	15.7	12.8	15.9	1.22	1.24
Trehalose	152.2	136.6	169.0	1.11	1.24
Alpha-Linolenic acid	167.9	170.4	210.0	0.99	1.23
Alanine	610.9	701.0	862.8	0.87	1.23
Linoleic acid	94.6	97.7	120.2	0.97	1.23
Arachidic acid	3.7	4.2	5.2	0.88	1.23
18.08 498 588 558	0.21	0.28	0.35	0.74	1.23*
Glycerol-2-phosphate	13.6	14.3	17.4	0.95	1.22
Alpha-Aminoadipic acid	18.8	17.5	21.4	1.07	1.22
Shikimic acid	1029.8	976.0	1188.1	1.06	1.22
Fructose	170.4	166.3	202.2	1.03	1.22
Glycolic acid	21.9	22.1	26.7	0.99	1.21
Ribitol	35.0	35.9	43.3	0.97	1.21
Salicylic acid-2-O-glucoside	5.8	5.2	6.2	1.12	1.20
Ferulic acid	2.8	3.0	3.6	0.95	1.20
Secoisolariciresinol	2.1	2.2	2.6	0.97	1.16
Ethyl-phosphate	195.2	209.7	242.4	0.93	1.16
Docosanoic acid	3.5	4.2	4.8	0.85	1.15
Serine	552.5	606.5	699.2	0.91	1.15
Citramalic acid	31.9	27.6	31.7	1.16	1.15
2-Hydroxyglutaric acid	30.7	26.5	30.4	1.16	1.15
5-Hydroxyferulic acid-glucoside	0.3	0.5	0.5	0.63	1.15
Adenine	10.8	11.5	13.2	0.94	1.15
5-Hydroxyferulic acid	0.8	1.0	1.1	0.86	1.14
Cholesterol	6.2	5.6	6.3	1.10	1.13
Tetracosanoic acid	15.4	19.4	21.8	0.79	1.13
Ascorbic acid	7.7	8.3	9.3	0.93	1.12
Maleic acid	67.4	69.5	78.1	0.97	1.12
Glycerol	529.6	529.1	590.8	1.00	1.12
Gamma-Tocopherol	1.3	1.4	1.5	0.92	1.11
Oleic acid	4.8	5.6	6.2	0.86	1.11
Phosphoethanolamine	14.4	15.3	16.8	0.94	1.09
Ethanolamine	2136.7	2576.2	2818.1	0.83*	1.09
Butyric acid	8.7	9.2	10.0	0.94	1.09
Arbutin	1.9	2.1	2.3	0.91	1.09
Galactose	390.0	445.0	482.9	0.88	1.09
Glutamine	550.3	771.9	836.2	0.71*	1.08
Aspartic acid	1042.3	1146.2	1240.7	0.91	1.08
B-alanine	79.6	102.5	110.2	0.78*	1.08

Please cite this article in press as: Zhao, Q., et al. Pinoresinol reductase 1 impacts lignin distribution during secondary cell wall biosynthesis in Arabidopsis. Phytochemistry (2014), http://dx.doi.org/10.1016/j.phytochem.2014.07.008

Table 1 (*continued*)

Plant type Metabolite	*prr1* Avg	WT Avg	PrR1 Avg	Fold change prr1/WT	Fold change PrR1/WT
Erythronic acid	180.4	178.0	190.8	1.01	1.07
Fumaric acid	4186.3	4022.3	4300.3	1.04	1.07
Myoinositol-2-phosphate	20.1	20.8	22.2	0.97	1.07
Stigmastanol	6.2	6.3	6.7	0.99	1.07
Phenylalanine	76.8	82.8	87.9	0.93	1.06
17.28 456 162 syringyl-guaiacyl lignan	6.5	6.9	7.3	0.95	1.06
Leucine	41.4	35.5	37.6	1.16	1.06
Syringaldehyde	2.2	2.7	2.8	0.82	1.06
Succinic acid	197.8	206.8	217.7	0.96	1.05
Palmitic acid	197.4	180.0	188.6	1.10	1.05
Glycerol-1/3-phosphate	177.0	182.0	190.0	0.97	1.04
Adenosine	29.2	35.4	36.7	0.83	1.04
Glucose	1410.1	1528.1	1581.5	0.92	1.03
Campesterol	63.4	72.3	74.7	0.88	1.03
Erythronic acid-gamma-lactone	203.7	200.7	207.5	1.01	1.03
Phytol	2253.1	2555.9	2629.1	0.88	1.03
Sitosterol	195.3	198.4	203.0	0.98	1.02
4-Hydroxybenzoic acid	5.3	5.7	5.8	0.94	1.02
3,4-Dihydroxybenzoic acid	2.5	2.3	2.4	1.06	1.02
Sinapoyl-malic acid	1.6	3.2	3.2	0.50*	1.01
17.56 453 468 209	0.29	0.40	0.41	0.71*	1.01
Isoleucine	47.0	48.1	48.7	0.98	1.01
Citric acid	473.1	538.2	544.5	0.88	1.01
1-(Indol-3-yl)-piperidinocyclopropane	3.7	3.5	3.6	1.04	1.01
Quinic acid	0.4	0.5	0.5	0.82	1.01
Threonine	367.7	487.3	487.3	0.75	1.00
B-amyrin	22.9	23.3	23.2	0.98	1.00
Sucrose	2513.4	2509.0	2485.8	1.00	0.99
Myoinositol	0.5	0.5	0.5	0.95	0.99
2-Hydroxy-2-propenoic acid	18.9	24.7	24.5	0.76	0.99
Tyrosine	25.3	22.9	22.6	1.11	0.99
cis-Sinapic acid-4-O-glucoside	0.7	0.8	0.8	0.88	0.98
2-Hydroxy-3-methylvaleric acid	176.2	209.9	204.7	0.84	0.98
Valine	196.0	236.4	226.3	0.83	0.96
Lysine	52.9	51.5	48.9	1.03	0.95
9.91 114 281 354 256 184	9.0	11.6	11.0	0.78*	0.95
Asparagine	66.3	90.8	86.1	0.73	0.95
1-Hexacosanol	11.9	14.4	13.5	0.83	0.94
Malic acid	724.3	785.0	732.7	0.92	0.93
Kaempferol	2.2	3.8	3.5	0.58	0.93
15-Nonacosanone	12.1	17.8	16.5	0.68	0.93
Benzoic acid	22.6	23.3	21.4	0.97	0.92
Salicylic acid	3.4	6.2	5.7	0.55	0.92
Aconitic acid	5.7	7.5	6.9	0.76	0.91
Tryptophan	30.7	29.4	26.6	1.04	0.90
Glyceric acid	231.6	281.3	253.9	0.82	0.90
Stearic acid	58.9	48.5	42.4	1.21	0.87
Pinoresinol	0.19	0.04	0.03	4.79*	0.85
Lactic acid	19.7	13.1	10.3	1.50	0.79
Nonacosane	20.0	32.9	25.7	0.61	0.78
3-Phosphoglyceric acid	5.4	8.4	6.5	0.64	0.77

* Designates that the fold change is statistically significant ($P \leqslant 0.05$) based on Student *t*-tests.

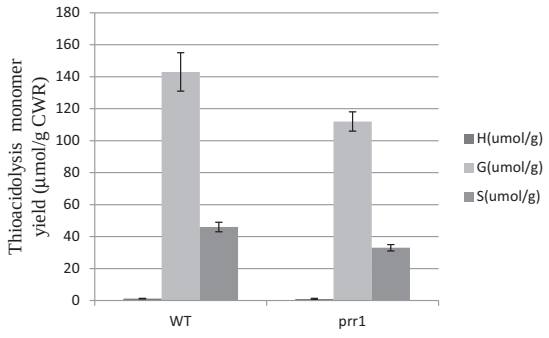

Fig. 3. Lignin thioacidolysis yields are reduced in the *prr1* mutant.

of the lignin monomer, coniferyl alcohol, gives rise to pinoresinol, a simple lignan with 9(9′)-oxygen linkages. Pinoresinol is then sequentially reduced to lariciresinol and secoisolariciresinol by a bi-functional pinoresinol/lariciresinol reductase (PLR) (Nakatsubo et al., 2008; Umezawa, 2003). *PLR*/*PrR* genes have organ-specific expression patterns. In Arabidopsis, PrR1and PrR2 redundantly catalyze the reduction of pinoresinol in roots. *PrR2* is root-specific and *PrR1* is expressed highly in both roots and aerial tissues (Nakatsubo et al., 2008). Pinoresinol levels in aerial tissue increase following loss of function of *PrR1*, indicating that *PrR1* plays a role in lignan biosynthesis in aerial tissue and has not, therefore, undergone complete neofunctionalization, and the observation that over-expression of PrR1 results in over-production of lignans other than lariciresinol indicates that the gene has a more generalized effect on lignan production than previously known. It is also interesting that both this study and a previous one (Ruprecht et al., 2011) show that lignin content is decreased when *PrR1* expression is disrupted. In fact, lignin content might be expected to be increased when lignan biosynthesis is compromised, considering the potential for competition between the lignin and lignan pathways.

Please cite this article in press as: Zhao, Q., et al. Pinoresinol reductase 1 impacts lignin distribution during secondary cell wall biosynthesis in Arabidopsis. Phytochemistry (2014), http://dx.doi.org/10.1016/j.phytochem.2014.07.008

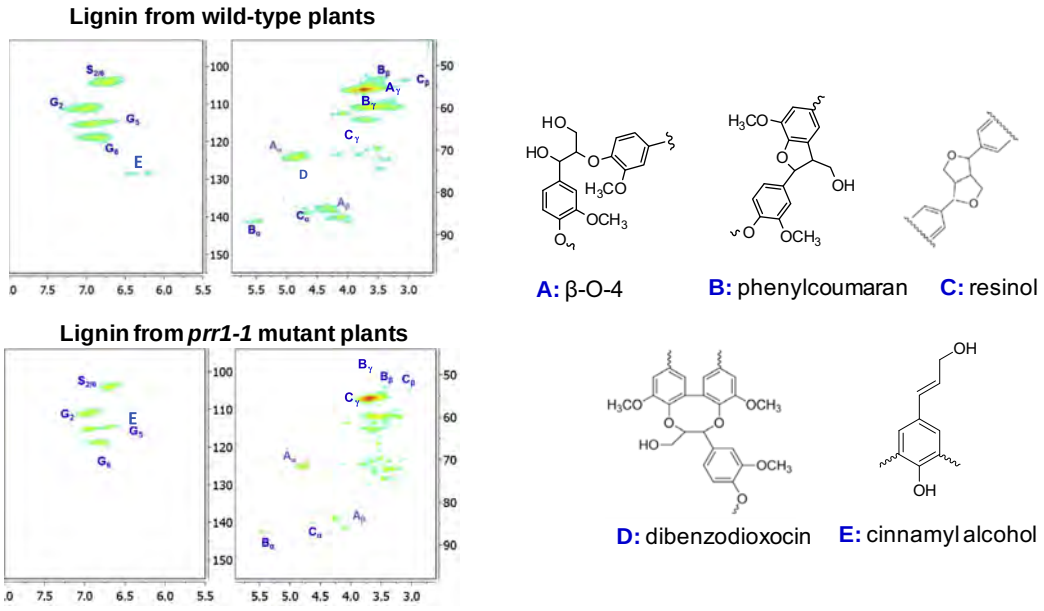

Fig. 4. ^{13}C–^{1}H HSQC spectra of lignin samples from wild type and *prr1* loss-of-function mutant. Each HSQC spectrum is split into two parts to expand the aromatic and aliphatic regions for clearer comparison. Lignin substructures are shown on the right.

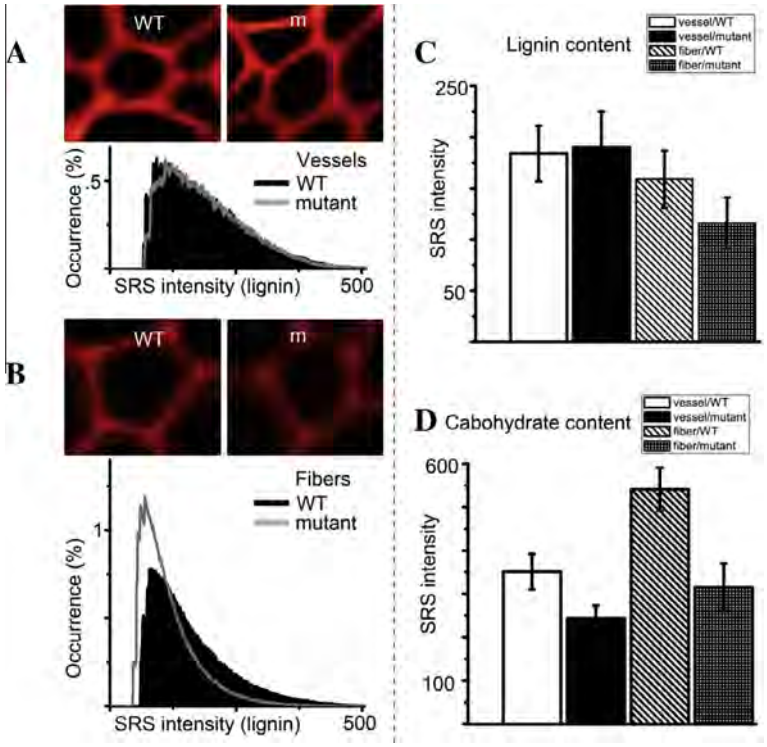

Fig. 5. Lignin and carbohydrate distribution and contents in xylem and fiber cells as revealed by two-color Stimulated Raman Scattering (SRS) microscopy. Similar signals are seen in xylem cells between the *prr1-1* mutant and wild type (A), but in fiber cells the lignin signal is lower and more narrowly distributed in the *prr1-1* mutant than in the wild type (B). (C) Lignin content comparison between wild type and *prr1-1* mutant. (D) Carbohydrate content comparison between wild type and *prr1-1* mutant.

Therefore, it is possible that lignan or "lignan-like" compounds may somehow be involved in lignin polymerization, consistent with the fact that *PrR1* is co-expressed with genes involved in secondary wall biosynthesis, especially the lignin laccase *LAC17*. No other lignin biosynthetic genes appear to co-express with *PrR1*, suggesting that the biosynthetic pathways to monolignols and lignans are independently regulated. Some types of lignans might be incorporated into lignin polymers with the help of the lignin laccase *LAC17*. However, with current technology, it is very hard to detect *in situ* lignan deposition into lignin polymers. Furthermore, it seems unlikely that initial formation of lignan-like units is an early critical step in lignin polymerization, because, unlike the dramatic loss of lignin phenotype observed in Arabidopsis following loss of function of the three laccase genes *LAC4*, *LAC11* and *LAC17* (Zhao et al., 2013a), loss of function of *PrR1* has only a small impact on lignin quantity.

Please cite this article in press as: Zhao, Q., et al. Pinoresinol reductase 1 impacts lignin distribution during secondary cell wall biosynthesis in Arabidopsis. Phytochemistry (2014), http://dx.doi.org/10.1016/j.phytochem.2014.07.008

This small reduction in overall lignin quantity, accompanied by altered lignin distribution across the walls of fiber cells, would not be expected to result in gross changes in vascular morphology, unless a critical sub-fraction of the lignin polymer were being affected. It is therefore not clear why a previous report indicated that loss of function of PrR1 results in an increased percentage of distorted xylem vessels in Arabidopsis (Ruprecht et al., 2011), an observation that we could not replicate under the growth conditions used in the present work.

Although lignans and lignins share the same building blocks, they are assembled differently. For example, lignin linkage formation mostly involves the 4-hydroxyl of monolignols, but the majority of lignan dimers are joined by β–β linkages (Weng and Chapple, 2010). Lignan dimerization is considered to be an enantioselective radical coupling reaction (Davin et al., 1997), in contrast to the overall achiral process of lignin polymerization. The different linkage types in lignans and lignins suggest that there may be different oxidase enzymes involved in the respective polymerization steps. Lignans appeared earlier than lignin during evolution of plants, as they can be found in some bryophytes (Scher et al., 2003; Umezawa, 2003), whereas no solid evidence supports the presence of lignin polymers in bryophytes (Weng and Chapple, 2010). Coincidently, a phylogenetic analysis of laccases indicated that the lignin-specific laccases appear to be seed-plant specific (Zhao et al., 2013a).

The occurrence of phenylpropanoid metabolism is considered to be critical in the initial move of the aquatic ancestors of current plants onto land. Even though sporadic literature reports indicate that the biosynthesis of lignin-like compounds can be tracked back to non-vascular plants, the presence of lignin in mosses is still an open question, not to mention aquatic algal species (Weng and Chapple, 2010). However, moss cell walls contain polysaccharides with very similar composition to those of vascular plants, even though there are only trace amounts of lignin attached (Roberts et al., 2012). This raises the possibility that, in non-vascular plants, lignans may have been integrated into cell walls before the appearance of lignin, and this may represent an early step towards the evolution of lignification of secondary cell walls. This could explain the co-expression of *PrR1* with secondary cell wall biosynthetic genes. Alternatively, association of lignans with cell walls could be viewed as a purely defensive function.

Recently, it has been shown that biosynthesis of lignans and oligolignols can accompany secondary cell wall biosynthesis in both angiosperms and gymnosperms (Huis et al., 2012; Villalobos et al., 2012). Furthermore, a study using lignan-derived antibodies immunolocalized lignans in the secondary walls in flaxseed (Attoumbre et al., 2010). Clearly, both quantitative and qualitative differences in lignin deposition are linked to disruption of a critical lignan biosynthetic gene, *PrR1*. Because Arabidopsis accumulates most lignans in root tissue, the root-specific gene *PrR2* is functionally redundant with *PrR1* in roots as regards to lignan biosynthesis (Nakatsubo et al., 2008), and we have here shown that PrR2 co-expresses with two genes potentially involved in casparian strip formation in the root, it will be interesting to investigate whether there are cell wall phenotypes in root tissue when both *PrR* genes are not functional.

4. Experimental

4.1. Plant growth conditions

Arabidopsis plants were grown in MetroMix 350 soil under 16 h light/8 h dark cycles at 23 °C during the day and 21 °C during the night 70–80% relative humidity, and 150 μmol m^{-2} s^{-1} light intensity.

4.2. Plant materials

The *prr1-1* mutant SALK_058467 and the *prr2-1* mutant SALK_123621 were obtained from the ABRC at Ohio State University (http://abrc.osu.edu/).

4.3. Determination of lignin composition

Mature stems from 6 week old plants were harvested for lignin analysis using previously published procedures (Zhao et al., 2013b).

4.4. Metabolite profiling analysis

Fast-frozen shoot samples of two replicates each of the *prr1-1* loss-of-function mutant, the PrR1 overexpressor line, and wild-type *A. thaliana* plants were freeze dried, ground with a micro-Wiley mill, and 46–68 mg (dry weight) of tissue twice extracted with 2.5 mL 80% ethanol overnight and then combined prior to drying a 3 mL aliquot in a nitrogen stream. Sorbitol was added (to achieve 103.45 ng/μL injected) before extraction as an internal standard to correct for differences in extraction efficiency, subsequent differences in derivatization efficiency and changes in sample volume during heating. Dried extracts were dissolved in 500 μL of silylation–grade acetonitrile followed by the addition of 500 μL N-methyl-N-trimethylsilyltrifluoroacetamide (MSTFA) with 1% trimethylchlorosilane (TMCS) (Thermo Scientific, Bellefonte, PA), and samples then heated for 1 h at 70 °C to generate trimethylsilyl (TMS) derivatives (Li et al., 2012; Tschaplinski et al., 2013). After 2 days, 1-μL aliquots were injected into an Agilent Technologies Inc. (Santa Clara, CA) 5975C inert XL gas chromatograph-mass spectrometer, fitted with an Rtx-5MS with Integra-guard (5% diphenyl/95% dimethyl polysiloxane) 30 m × 250 μm × 0.25 μm film thickness capillary column. The standard quadrupole GC–MS was operated in the electron impact (70 eV) ionization mode, targeting 6 full-spectrum (50–650 Da) scans per second. Gas (helium) flow was set at 1.0 mL per minute with the injection port configured in the splitless mode. The injection port, MS Source, and MS Quad temperatures were set to 250 °C, 230 °C, and 150 °C, respectively. The initial oven temperature was held at 50 °C for 2 min and was programmed to increase at 20 °C per min to 325 °C and held for another 11 min, before cycling back to the initial conditions. A total of 170 metabolite peaks were extracted using a key selected ion, characteristic *m*/*z* fragment, rather than the total ion chromatogram, to minimize integrating co-eluting metabolites. The extracted peaks of known metabolites were scaled back up to the total ion current using predetermined scaling factors. Peaks were quantified by area integration and the concentrations were normalized to the quantity of the internal standard (sorbitol) recovered, amount of sample extracted, derivatized, and injected. A large user-created database (>1900 spectra) of mass spectral electron impact ionization (EI) fragmentation patterns of TMS-derivatized compounds, as well as the Wiley Registry 8th Edition combined with NIST 05 mass spectral database, were used to identify the metabolites of interest to be quantified. Student's *t*-tests were used to test for significant differences ($P \leqslant 0.05$) between the mutant lines and the wild-type controls.

4.5. Transfection of leaf protoplasts for transactivation analysis

Leaves from 4 week-old greenhouse-grown *Arabidopsis* were used as a source of protoplasts. One reporter construct (promoter-luciferase) and one effector construct (35S: transcription factor) were co-transfected into protoplasts as described (Zhao et al., 2010b). A reference construct containing the Renilla luciferase gene driven by the 35S promoter was also co-transfected to

Please cite this article in press as: Zhao, Q., et al. Pinoresinol reductase 1 impacts lignin distribution during secondary cell wall biosynthesis in Arabidopsis. Phytochemistry (2014), http://dx.doi.org/10.1016/j.phytochem.2014.07.008

determine the transfection efficiency. Luciferase activities were determined using the dual-luciferase reporter assay system (Promega, Madison, WI). The firefly luciferase activity was calculated by normalizing against the Renilla luciferase activity in each transfection event. Data are presented as averages ± SE of three biological replicates.

4.6. Sample preparation for microscopy

Wild-type and mutant plants were grown in the greenhouse. The second internodes were used for microscopic analysis. The stem was hand cut into approximately 50 μm thickness slices. All samples were washed with distilled water several times and imaged in water.

4.7. SRS microscopy

The two-color Stimulated Raman Scattering (SRS) imaging microscope using a mode-locked Nd:YVO_4 laser (High Q Laser, Austria) was used to generate a 7 ps, 76 MHz pulse train of both 1064 nm (1 W average power) and 532 nm (5 W average power) laser beams. The 1064 nm output was used as the Stokes light. The 532 nm beam was 50/50 split to pump two optical parametric oscillators (OPO) (Levante Emerald, A·P·E Angewandte Physik und Elektronik GmbH, Berlin). The output wavelengths of the OPOs were selected at 812 and 909 nm to use as pump beams to induce the Stimulated Raman signal for the 2900 cm^{-1} carbohydrate C–H vibration and the 1600 cm^{-1} lignin aromatic ring vibration, respectively. All pump and Stokes beams were directed into an Olympus laser scanning microscope scanning unit (BX62WI/FV300, Olympus) and focused by a high numerical aperture water-immersion objective (UPLSApo 60X 1.20 NA W, Olympus). The light transmitted through the sample was collected by an oil-immersion condenser (1.45 NA O, Nikon). The stimulated Raman loss signals were detected by silicon PIN photodiodes (FDS1010, Thorlabs) and a lock-in amplifier (SR844, Stanford Research Systems) as previously described (Ding et al., 2012).

4.8. Image analysis

Intensity analysis for specific types of cell wall was performed in MATLAB (MATLAB R2012b) with user-written scripts. Multiple regions containing no cell wall components were manually selected across the image of interest, which were used to determine the background intensity. The mean background intensity plus three times background intensity standard deviation was used as a threshold. The program then selected pixels with intensity value above the threshold for statistical analysis. For each type of plant sample, 5 images containing ~50 cells were selected for intensity analysis. Lignin (1600 cm^{-1}) and carbohydrate (2900 $cm^{-1)}$ signals in each pixel were plotted, respectively, as intensity histograms and normalized by total intensity for better comparison.

4.9. Lignin isolation and NMR analysis

The lignin samples for NMR spectroscopy analysis were prepared according to a slightly modified cellulolytic enzyme lignin isolation procedure as previously described (Chang et al., 1975; Holtman et al., 2004). In brief, the Arabidopsis samples from prr1 knout-out and WT lines were extracted with toluene/ethanol (2:1, v/v) for 24 h. The extractive-free cell walls were ball-milled using a planetary ball mill (Retsch PM 100) in a 50 mL ZrO_2 vessel at 600 rpm with 10 min break after every 5 min of milling. The ball-milled powder samples were then subjected to enzyme treatment in acetic acid/ammonium acetate buffer (pH 4.8) with cellulase and β-glucosidase for 2 × 48 h at 50 °C under continuous agitation at 200 rpm. The residue was isolated by centrifugation, washed with deionized water, and freeze dried. The enzyme-treated residue was extracted with dioxane–water (96:4 v/v) for 24 h × 2. The mixtures were centrifuged and the supernatant was collected, roto-evaporated at 40 °C under reduced pressure, and freeze-dried.

NMR spectra were acquired using a Bruker Avance-III 400 MHz spectrometer operating at a frequency of 100.59 MHz for ^{13}C nucleus. Deuterated dimethyl sulfoxide (DMSO) was used as solvent for lignin samples. The ^{13}C–^{1}H HSQC correlation spectra were recorded using a Bruker standard pulse sequence ('hsqcetgpsi2') with the following acquisition parameters: 10-ppm spectra width in F2 (^{1}H) dimension with 2048 data points (256 ms acquisition time), 210-ppm spectra width in F1 (^{13}C) dimension with 320 data points (7.6 ms acquisition time), a 1.0-s pulse delay, and a $^{1}J_{CH}$ of 145 Hz (Moinuddin et al., 2010; Pu et al., 2009). The number of scans were 256 for the WT and 350 for the PrR mutant. The central solvent peak (δ_C 39.5 ppm; δ_H 2.5 ppm) was used for chemical shift calibration. NMR data were processed using the TopSpin 2.1 (Bruker BioSpin) and MestreNova (Mestre Labs) software packages.

4.10. DNA microarray analysis

Total RNA was isolated from mature inflorescences of 6-week-old plants with Tri-reagent using the manufacturer's protocol (Invitrogen, http://www.invitrogen.com). RNA was cleaned and concentrated using the RNeasy MinElute Cleanup Kit (Qiagen, http://www.qiagen.com), and 500 ng of purified RNA used for microarray analysis of three biological replicates of *prr1* mutant and control plants. Probe labeling, hybridization and scanning were conducted according to the manufacturer's instructions (Affymetrix, http://www.affymetrix.com). Data normalization used robust multi-chip average (RMA) and the presence/absence call for each probe set was obtained from dCHIP (Li and Wong, 2001). Genes with significantly different expression levels between the wild-type control and mutants were selected using associative analysis (Dozmorov and Centola, 2003), and the type-I family-wise error rate was reduced by using a Bonferroni-corrected *P*-value threshold of 0.05/*N*, where *N* represents the number of genes present on the chip. The false discovery rate was monitored and controlled by *Q* value (false discovery rate), calculated using Extraction of Differential Gene Expression (Leek et al., 2006).

Acknowledgements

This paper is dedicated to the memory of G. Paul Bolwell. We thank Dr. Yuhong Tang for assistance with DNA microarray analysis. This work was supported by the Samuel Roberts Noble Foundation (OKlahoma, United States) and the BioEnergy Science Center, a U.S. Department of Energy Bioenergy Research Center supported by the Office of Biological and Environmental Research in the DOE Office of Science. This manuscript has been authored by a contractor of the U.S. Government under contract DE-AC05-00OR22725.

Appendix A. Supplementary data

Supplementary data associated with this article can be found, in the online version, at http://dx.doi.org/10.1016/j.phytochem.2014.07.008.

References

Attoumbre, J., Bienaime, C., Dubois, F., Fliniaux, M.A., Chabbert, B., Baltora-Rosset, S., 2010. Development of antibodies against secoisolariciresinol – application to the immunolocalization of lignans in *Linum usitatissimum* seeds. Phytochemistry 71, 1979–1987.

Berthet, S., Demont-Caulet, N., Pollet, B., Bidzinski, P., Cezard, L., Le Bris, P., Borrega, N., Herve, J., Blondet, E., Balzergue, S., Lapierre, C., Jouanin, L., 2011. Disruption of LACCASE4 and 17 results in tissue-specific alterations to lignification of *Arabidopsis thaliana* stems. Plant Cell 23, 1124–1137.

Binns, A.N., Chen, R.H., Wood, H.N., Lynn, D.G., 1987. Cell division promoting activity of naturally occurring dehydrodiconiferyl glucosides: do cell wall components control cell division? Proc. Natl. Acad. Sci. U.S.A. 84, 980–984.

Bonawitz, N.D., Chapple, C., 2010. The genetics of lignin biosynthesis: connecting genotype to phenotype. Annu. Rev. Genet. 44, 337–363.

Chang, H.-M., Cowling, E.B., Brown, W., Adler, E., Miksche, G., 1975. Comparative studies on cellulolytic enzyme lignin and milled wood lignin of sweetgum and spruce. Holzforschung 29, 153–159.

Davin, L.B., Wang, H.B., Crowell, A.L., Bedgar, D.L., Martin, D.M., Sarkanen, S., Lewis, N.G., 1997. Stereoselective bimolecular phenoxy radical coupling by an auxiliary (dirigent) protein without an active center. Science 275, 362–366.

Davis, J., Brandizzi, F., Liepman, A.H., Keegstra, K., 2010. Arabidopsis mannan synthase CSLA9 and glucan synthase CSLC4 have opposite orientations in the Golgi membrane. Plant J. 64, 1028–1037.

Ding, S.Y., Liu, Y.S., Zeng, Y.N., Himmel, M.E., Baker, J.O., Bayer, E.A., 2012. How does plant cell wall nanoscale architecture correlate with enzymatic digestibility? Science 338, 1055–1060.

Dixon, R.A., 2004. Phytoestrogens. Annu. Rev. Plant Biol. 55, 225–261.

Dozmorov, I., Centola, M., 2003. An associative analysis of gene expression array data. Bioinformatics 19, 204–211.

Hano, C., Martin, I., Fliniaux, O., Legrand, B., Gutierrez, L., Arroo, R.R., Mesnard, F., Lamblin, F., Laine, E., 2006. Pinoresinol-lariciresinol reductase gene expression and secoisolariciresinol diglucoside accumulation in developing flax (*Linum usitatissimum*) seeds. Planta 224, 1291–1301.

Hemmati, S., von Heimendahl, C.B., Klaes, M., Alfermann, A.W., Schmidt, T.J., Fuss, E., 2010. Pinoresinol-lariciresinol reductases with opposite enantiospecificity determine the enantiomeric composition of lignans in the different organs of *Linum usitatissimum* L. Planta Med. 76, 928–934.

Holtman, K.M., Chang, H.-M., Kadla, J.F., 2004. Solution-state nuclear magnetic resonance study of the similarities between milled wood lignin and cellulolytic enzyme lignin. J. Agric. Food Chem. 52, 720–726.

Huis, R., Morreel, K., Fliniaux, O., Lucau-Danila, A., Fenart, S., Grec, S., Neutelings, G., Chabbert, B., Mesnard, F., Boerjan, W., Hawkins, S., 2012. Natural hypolignification is associated with extensive oligolignol accumulation in flax stems. Plant Physiol. 158, 1893–1915.

Lee, Y., Rubio, M.C., Alassimone, J., Geldner, N., 2013. A mechanism for localized lignin deposition in the endodermis. Cell 153, 402–412.

Leek, J.T., Monsen, E., Dabney, A.R., Storey, J.D., 2006. EDGE: extraction and analysis of differential gene expression. Bioinformatics 22, 507–508.

Li, C., Wong, W.H., 2001. Model-based analysis of oligonucleotide arrays: expression index computation and outlier detection. Proc. Natl. Acad. Sci. U.S.A. 98, 31–36.

Li, Y., Tschaplinski, T.J., Engle, N.L., Hamilton, C.Y., Rodriguez Jr., M., Liao, J.C., Schadt, C.W., Guss, A.M., Yang, Y., Graham, D.E., 2012. Combined inactivation of the *Clostridium cellulolyticum* lactate and malate dehydrogenase genes substantially increases ethanol yield from cellulose and switchgrass fermentations. Biotechnol. Biofuels 5, 2.

McCann, M.J., Gill, C.I., McGlynn, H., Rowland, I.R., 2005. Role of mammalian lignans in the prevention and treatment of prostate cancer. Nutr. Cancer 52, 1–14.

Moinuddin, S.G.A., Jourdes, M., Laskar, D.D., Ki, C., Cardenas, C.L., Kim, K.W., Zhang, D., Davin, L.B., Lewis, N.G., 2010. Insights into lignin primary structure and deconstruction from *Arabidopsis thaliana* COMT (caffeic acid O-methyl transferase) mutant Atomt1. Org. Biomol. Chem. 8, 3928–3946.

Nakashima, J., Chen, F., Jackson, L., Shadle, G., Dixon, R.A., 2008. Multi-site genetic modification of monolignol biosynthesis in alfalfa (*Medicago sativa* L.) – effects on lignin composition in specific cell types. New Phytol. 179, 738–750.

Nakatsubo, T., Mizutani, M., Suzuki, S., Hattori, T., Umezawa, T., 2008. Characterization of *Arabidopsis thaliana* pinoresinol reductase, a new type of enzyme involved in lignan biosynthesis. J. Biol. Chem. 283, 15550–15557.

Naoumkina, M.A., Zhao, Q., Gallego-Giraldo, L., Dai, X., Zhao, P.X., Dixon, R.A., 2010. Genome-wide analysis of phenylpropanoid defence pathways. Mol. Plant Pathol. 11, 829–846.

Pu, Y., Chen, F., Ziebell, A., Davison, B.H., Ragauskas, A.J., 2009. NMR characterization of C3H and HCT down-regulated alfalfa lignin. Bioenergy Res. 2, 198–208.

Roberts, A.W., Roberts, E.M., Haigler, C.H., 2012. Moss cell walls: structure and biosynthesis. Front. Plant Sci. 3, 166.

Ruprecht, C., Mutwil, M., Saxe, F., Eder, M., Nikoloski, Z., Persson, S., 2011. Large-scale co- expression approach to dissect secondary cell wall formation across plant species. Front. Plant Sci. 2, 23.

Scher, J.M., Zapp, J., Becker, H., 2003. Lignan derivatives from the liverwort *Bazzania trilobata*. Phytochemistry 62, 769–777.

Schmidt, T.J., Hemmati, S., Klaes, M., Konuklugil, B., Mohagheghzadeh, A., Ionkova, I., Fuss, E., Wilhelm Alfermann, A., 2010. Lignans in flowering aerial parts of Linum species – chemodiversity in the light of systematics and phylogeny. Phytochemistry 71, 1714–1728.

Tschaplinski, T.J., Standaert, R.F., Engle, N.L., Martin, M.Z., Sangha, A.K., Parks, J.M., Smith, J.C., Samuel, R., Pu, Y., Ragauskas, A.J., Hamilton, C.Y., Fu, C., Wang, Z.-Y., Davison, B.H., Dixon, R.A., Meilenz, J.R., 2013. Down-regulation of the caffeic acid *O*-methyltransferase gene in switchgrass reveals a novel monolignol analog. Biotechnol. Biofuels 5, 71.

Umezawa, T., 2003. Diversity in lignan biosynthesis. Phytochem. Rev. 2, 371–390.

Villalobos, D.P., Diaz-Moreno, S.M., Said el, S.S., Canas, R.A., Osuna, D., Van Kerckhoven, S.S., Bautista, R., Claros, M.G., Canovas, F.M., Canton, F.R., 2012. Reprogramming of gene expression during compression wood formation in pine: coordinated modulation of S-adenosylmethionine, lignin and lignan related genes. BMC Plant Biol. 12, 100.

von Heimendahl, C.B., Schafer, K.M., Eklund, P., Sjoholm, R., Schmidt, T.J., Fuss, E., 2005. Pinoresinol-lariciresinol reductases with different stereospecificity from *Linum album* and *Linum usitatissimum*. Phytochemistry 66, 1254–1263.

Wang, S., Yin, Y., Ma, Q., Tang, X., Hao, D., Xu, Y., 2012. Genome-scale identification of cell-wall related genes in Arabidopsis based on co-expression network analysis. BMC Plant Biol. 12, 1–12.

Weng, J.K., Chapple, C., 2010. The origin and evolution of lignin biosynthesis. New Phytol. 187, 273–285.

Zhao, Q., Dixon, R.A., 2011. Transcriptional networks for lignin biosynthesis: more complex than we thought? Trends Plant Sci. 16, 227–233.

Zhao, Q., Gallego-Giraldo, L., Wang, H., Zeng, Y., Ding, S.Y., Chen, F., Dixon, R.A., 2010a. An NAC transcription factor orchestrates multiple features of cell wall development in *Medicago truncatula*. Plant J. 63, 100–114.

Zhao, Q., Nakashima, J., Chen, F., Yin, Y., Fu, C., Yun, J., Shao, H., Wang, X., Wang, Z.Y., Dixon, R.A., 2013a. LACCASE is necessary and nonredundant with PEROXIDASE for lignin polymerization during vascular development in Arabidopsis. Plant Cell 25, 3976–3987.

Zhao, Q., Tobimatsu, Y., Zhou, R., Pattathil, S., Gallego-Giraldo, L., Fu, C., Jackson, L.A., Hahn, M.G., Kim, H., Chen, F., Ralph, J., Dixon, R.A., 2013b. Loss of function of cinnamyl alcohol dehydrogenase 1 leads to unconventional lignin and a temperature-sensitive growth defect in *Medicago truncatula*. Proc. Natl. Acad. Sci. U.S.A. 110, 13660–13665.

Zhao, Q., Wang, H., Yin, Y., Xu, Y., Chen, F., Dixon, R.A., 2010b. Syringyl lignin biosynthesis is directly regulated by a secondary cell wall master switch. Proc. Natl. Acad. Sci. U.S.A. 107, 14496–14501.

Zhong, R., Demura, T., Ye, Z.H., 2006. SND1, a NAC domain transcription factor, is a key regulator of secondary wall synthesis in fibers of Arabidopsis. Plant Cell 18, 3158–3170.

Zhong, R., Richardson, E.A., Ye, Z.H., 2007. The MYB46 transcription factor is a direct target of SND1 and regulates secondary wall biosynthesis in Arabidopsis. Plant Cell 19, 2776–2792.

Please cite this article in press as: Zhao, Q., et al. Pinoresinol reductase 1 impacts lignin distribution during secondary cell wall biosynthesis in Arabidopsis. Phytochemistry (2014), http://dx.doi.org/10.1016/j.phytochem.2014.07.008